Direct Determination of Burning Velocity during Aluminium Flame Propagation

Clément Chanut, Frederic Heymes, Christian Lopez

CHEMICAL ENGINEERING TRANSACTIONS
VOL. 90, 2022
A publication of AIDIC
The Italian Association of Chemical Engineering
Online at www.cetjournal.it
Guest Editors: Aleš Bernatík, Bruno Fabiano

ISBN 978-88-95608-88-4; **ISSN** 2283-9216
DOI: 10.3303/CET2290065

Direct Determination of Burning Velocity during Aluminium Flame Propagation

Clement Chanut*, Frederic Heymes, Christian Lopez

Laboratoire des Sciences des Risques, IMT Mines Ales, Ales, France
clement.chanut@mines-ales.fr

Numerical simulations are needed to model accurately the consequences of dust explosions. One key parameter for modelling the flame propagation is the burning velocity (ie the consumption rate of the reactants by the flame front). Most of the methods used for experimentally determining this burning velocity are based on rough assumptions. In this paper, the determination of burning velocity during aluminium flame propagation is directly determined by the measurement of two velocities: the flame propagation velocity (ie flame front velocity in the laboratory referential) and the unburned flow velocity. Data of unburned flow velocity are obtained by Pitot tube and PIV (Particle Image Velocimetry) and are fairly close. An increase of burning velocity during aluminium flame propagation in the tube is observed. This increase is probably due to an increase of the turbulent intensity in front of the flame front during the propagation.

1. Introduction

Dust explosion is a major hazard in industries dealing with dusts and powders. To predict the consequences of an explosion, phenomena of flame propagation has to be modelled. Several models exist to predict the consequences of gas explosions. These models are used in some studies to predict consequences of dust explosions. These models seem adapted to predict some explosions involving organic dusts, but they are not accurate in case of metallic dusts (Kahlili, 2012). One key parameter used for flame propagation modelling is the burning velocity. This quantity represents the spatial consumption rate of the reactants by the flame front. Experiments are thus mandatory to estimate this burning velocity during metallic dust flame propagation.
Measurement of this burning velocity, especially for metallic flames, is a challenging experimental topic. Some studies focus on the determination of burning velocity by studying stationary flames with burners (Goroshin et al., 1996; Julien et al., 2017). With this setup, no data is obtained on the burning velocity during flame propagation. Other studies use data of confined explosions, frequently inside the 20-liter explosion sphere, to deduce burning velocity from pressure data (Dahoe & de Goey, 2003). A lot of assumptions are needed for determining the burning velocity from the pressure data, as highlighted by Faghih and Chen (2016). In the present study, experiments are performed in a vertical tube and propagating flames are studied to determine burning velocity. The main advantage of this setup is to obtain the evolution of burning velocity over time during the propagation of the flame front.
From images of flame propagation in a tube, burning velocity can be determined. In general, the so-called “open-tube method” is used to determine burning velocity from the propagation velocity (ie the velocity of the flame front in the laboratory referential) and the visualization of the flame shape. The main limit of this method is the estimation of the thermal expansion: this thermal expansion of the burned mixture is approximated by the value obtained for an adiabatic flame. Details of this method and of this limitation can be found in Chanut et al. (2020b).
A new method, called the “direct method”, has been proposed on this same previous paper based on the works of (Proust, 2006). This method is based on the direct measurement of two velocities: the propagation velocity and the unburned flow velocity. The difference between these two values is the burning velocity. In the previous paper a local measurement of this burning velocity was proposed, based on the measurement of the unburned flow velocity just ahead the flame front by PIV (Particle Image Velocimetry).

Paper Received: 26 January 2022; Revised: 24 March 2022; Accepted: 25 April 2022
Please cite this article as: Chanut C., Heymes F., Lopez C., 2022, Direct determination of burning velocity during aluminium flame propagation, Chemical Engineering Transactions, 90, 385-390 DOI:10.3303/CET2290065

In this paper, an adaptation of the previous method is proposed to estimate the global evolution of this burning velocity over time during aluminium flame propagation. In fact, the previous method proposed to study locally the burning velocity while this adaptation proposes to study the evolution over time of this burning velocity by a global estimation. For modelling and validation purpose, a simultaneous global estimation of the evolution of the propagation velocity, of the unburned flow velocity and of the burning velocity over time is of interest.

2. Materials and Methods

For this study, the prototype previously described in details in Chanut et al. (2020a) is adapted. This prototype is a vertical tube divided in three sections. Each section is a vertical tube of 700 mm height and 150 x 150 mm square cross section. Three walls of this prototype are made of glass to allow the visualization of flame propagation. Aluminium dust is injected in the prototype by discharging two compressed air vessels through four injection tubes located in the corners of the prototype. In general, aluminium is only injected on the first section. Injecting aluminium dust only on this first section is enough to produce a flame propagating up to the top of the third section. For the test presented hereafter, 3 g of aluminium dust are inserted in each of the four injection tubes of the first section resulting in a concentration of about 500 $g.m^{-3}$. After an adjustable delay (one second for the test presented hereafter), aluminium dust cloud is ignited by an electric spark between two electrodes located at the middle of the first section of the prototype. The energy of the spark is 300 J. The spark duration is 1 s. After ignition, flame propagates upward from the closed bottom end of the prototype to the open upper end. Aluminium studied has a mean diameter of 6.5 µm.

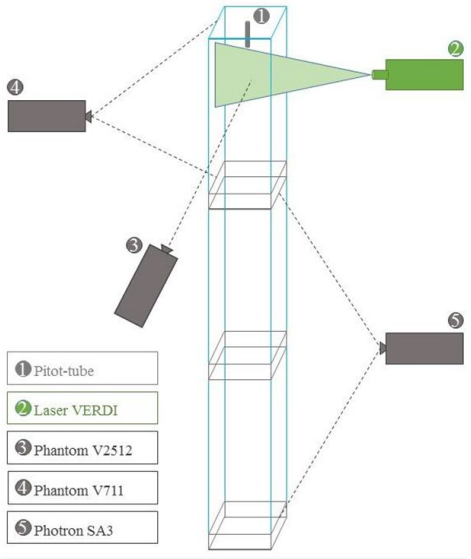

Figure 1: Schema of configuration for measuring propagation velocity and unburned flow velocity

Configuration implemented for measuring propagation velocity and unburned flow velocity is schematized on Figure 1. Two high-speed cameras are used to visualize the flame front propagation and to deduce the propagation velocity from the images obtained. The Photron SA3 camera records the flame propagation in the two first sections. This high-speed camera is equipped with a Nikkor 17-30 mm lens with an aperture of f/11. The exposure time is 2 µs. The acquisition rate is 10 000 fps (frames per second) corresponding to a resolution of 1024 x 128 pixels. The Phantom V711 camera focuses on the flame propagation in the third section. The lens mounted on this camera is a Nikkor 50 mm, with an aperture of f/16. The exposure time is 0.5 µs. The acquisition rate is 25 000 fps, corresponding to a resolution of 1280 x 232 pixels.
Two different measurement techniques are used to determine the unburned flow velocity. PIV (Particle Image Velocimetry) is the first measurement technique used to determine the unburned flow velocity. PIV measurement zone is located at the top of the third section just below the Pitot tube location. This setup consists on a continuous laser illuminating a plane of the flow and a high-speed camera recording the movements of particles in this plane. The laser is a continuous VERDI laser with a power of 5 W (wavelength: 532 nm). The high-speed camera is a Phantom V2512. The lens is a Nikkor 70-300 mm with an aperture of f/4. The exposure time is 5 µs. The acquisition rate is 25 000 fps corresponding to a resolution of 1280 x 800 pixels. 2D velocity maps are deduced from the images obtained using the DynamicStudio software (Dantec

Dynamics). For this analysis, the grid step size of the PIV algorithm is 16 x 16 pixels (spatial resolution). The PIV algorithm is an adaptative algorithm selecting the size of the interrogation window depending on the seeding and on the velocity field. For this analysis, the size of each interrogation window could be adapted from 8 to 32 pixels in each direction. For PIV measurements, flow has to be seeded with particles. For this purpose, aluminium particles are also dispersed in the second section. However, less dust is injected compared to the first section to improve the quality of the PIV images; 0.3 g of aluminium dust is injected on each of the four injection tubes of the second section.
The second measurement technique used for determining the unburned flow velocity is a Pitot tube located at the top of the third section. From the difference of pressure measured by this Pitot tube the unburned flow velocity is directly deduced from Eq(1):

$$v = \sqrt{\frac{2.\Delta P}{\rho}} \tag{1}$$

where v represents the unburned flow velocity calculated, ΔP is the pressure difference measured by the Pitot tube and ρ is the estimated density of the flow. For the determination of the mixture density, we considered air as an ideal gas at the room temperature and pressure; influence of particles on density is neglected (the dust suspension is less dense in the second section). Applying the ideal gas law, a density of 1,2 kg/m^3 is obtained. The recording frequency of the Pitot tube is 1 kHz.
With this setup, flame propagation and unburned flow velocities are measured. These two velocities are defined as upwards velocities; they are thus collinear. Therefore, the burning velocity is defined as the difference between these two velocities.

3. Results

3.1 Determination of propagation velocity

Aluminium flame propagation process is recorded by two high speed cameras. From the images obtained, the flame contour is extracted. The height of the flame front is then defined as the highest point of the detected contour. Figure 2 exhibits an example of an image obtained with the camera V711. The right image is a zomm of the left image, focusing on the flame front.The red line corresponds to the deduced flame height.

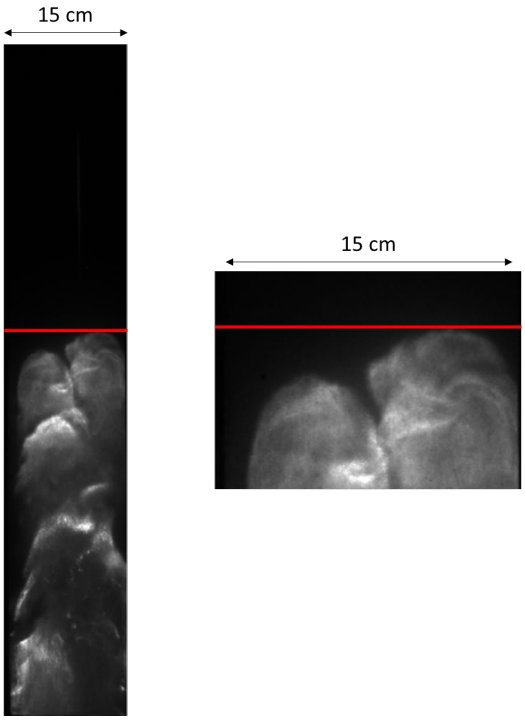

Figure 2. On the left: Example of an image of flame propagation obtained with the Phantom V711 (third section). On the right: zoom on the flame front (red line: locatio of the flame front height)

Evolution of this flame height over time, while the flame front is propagating inside the two upper sections, is exposed on Figure 3. This evolution is approximated with a second-order polynomial, exhibiting a flame propagating at a constant acceleration of around 280 $m.s^{-2}$, and thus a linear increase of the propagation velocity from 6 $m.s^{-1}$ (entry in the second section) to 28 $m.s^{-1}$ (flame in the third section).

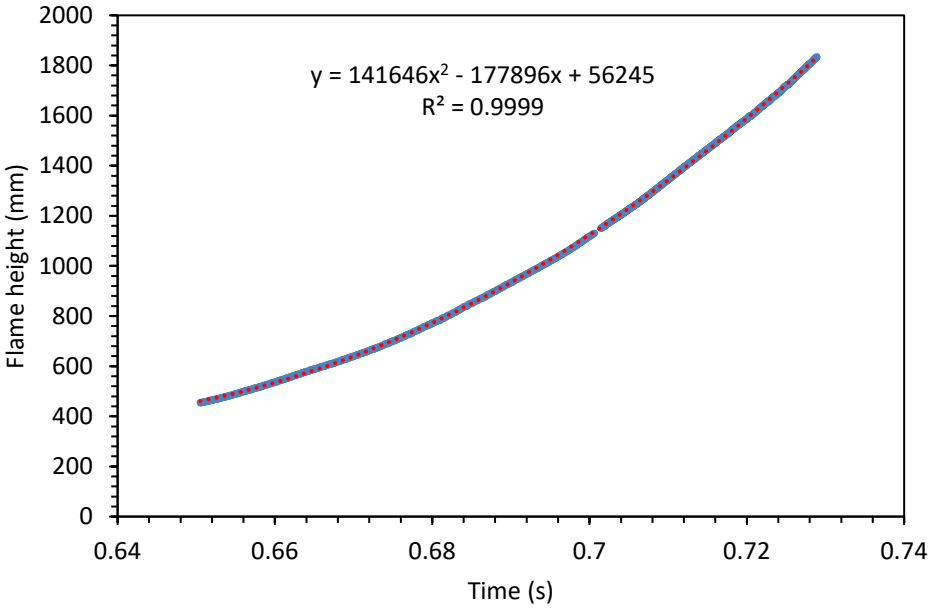

Figure 3: Evolution of flame height over time

3.2 Determination of unburned flow velocity

Unburned flow velocity is determined by two independent techniques: a Pitot tube and a PIV setup. From the Pitot tube, with the determination of the density exposed on the previous part, flow velocity is directly determined.

After PIV analysis, 2D maps of 2-component velocity vectors are obtained. The upward unburned flow velocity is defined as the spatial mean of the upward component of the velocity vectors in the part of the PIV field of view just above the Pitot tube. The location of this zone is exposed on Figure 4 with the corresponding number of interrogation windows (IW) in each direction used for the calculation of this mean upward velocity.

Evolutions of unburned flow velocity obtained with the Pitot tube and the PIV techniques are compared on Figure 5. These evolutions are studied only when the flame front is propagating in the two upper section to be consistent with the flame propagation velocity analysis. These evolutions are not exposed for $t > 0.71$ s, because after this time the flame luminosity disturbs the PIV measurements. The unburned flow velocities obtained with these two techniques are fairly close even if the evolution with the Pitot tube exhibits more fluctuations.

The ability of aluminum particles to follow the flow fluctuations is thus investigated. The period of the fluctuations observed by Pitot tube is around 25 ms. The corresponding Stokes number for these particles is 8 000. Based on the works of Mendez et al. (2018), considering the density of the aluminum particles, these particles are able to follow fluctuations with a period of 25 ms without attenuations. The difference between Pitot tube and PIV results is thus not due to the ability of the aluminium particles to follow these fluctuations.

These two velocity evolutions are well fitted by linear regressions, corresponding to a linear increase of the unburned flow velocity over time.

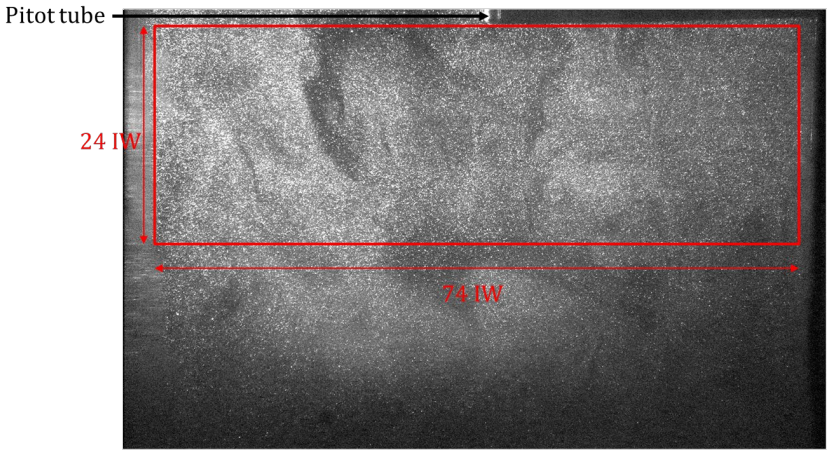

Figure 4: PIV images and field of view analyzed for determining the mean flow velocity

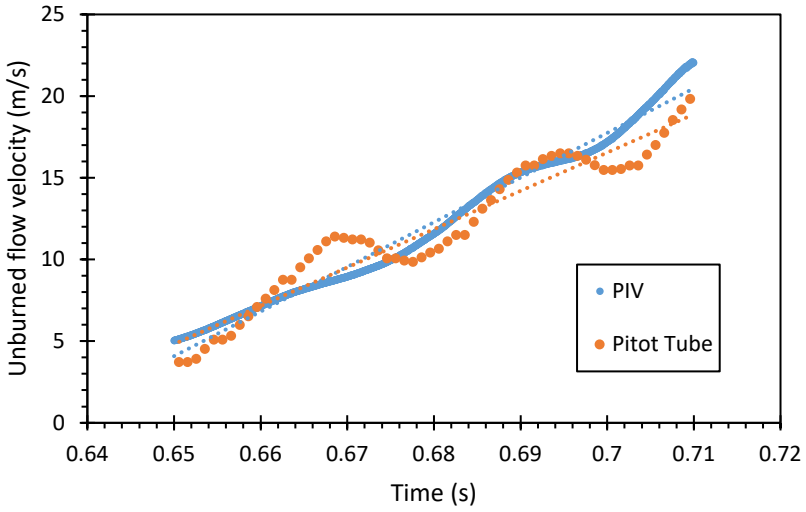

Figure 5: Evolution of unburned flow velocity. Comparison of PIV and Pitot tube results

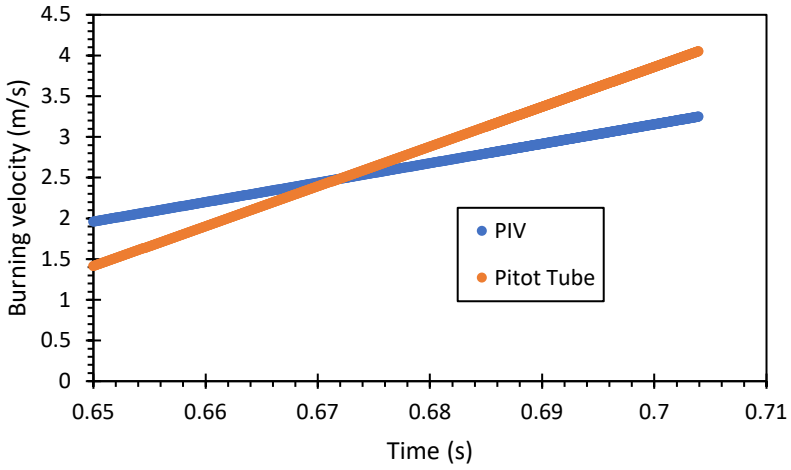

Figure 6: Evolution of burning velocity. Comparison of PIV and Pitot tube results

3.3 Determination of burning velocity

Burning velocity is then calculated as the difference between propagation velocity and unburned flow velocity. Linear fits of propagation velocity and unburned flow velocity are used to estimate the global evolution of the burning velocity. Evolutions of burning velocity depending on the technique used for unburned flow velocity determination are exposed on Figure 6. An increase of the burning velocity is observed from around 1.8 $m.s^{-1}$ to 3.5 $m.s^{-1}$. This increase of burning velocity can be due to an increase of the turbulent intensity ahead the flame front while the flame propagates in the tube.

4. Conclusions

A method has been proposed to estimate the evolution of the burning velocity over time during flame propagation in a tube. Contrary to other methods such as the “open-tube method”, this direct method is not based on an approximation of the flame temperature. With this method, the burning velocity is deduced from the measurement of two velocities: the propagation velocity and the unburned flow velocity.

In this paper, unburned flow velocity is determined by two independent techniques: a Pitot tube and a PIV setup. The velocities obtained by these two techniques are fairly close. The flame propagates with a constant acceleration corresponding to an increase of velocity from 6 $m.s^{-1}$ while the flame reaches second section to a velocity of 28 $m.s^{-1}$ when the flame is on the third section. Burning velocity increases while the fame is propagating in these two upper sections; from around 1.8 $m.s^{-1}$ to 3.5 $m.s^{-1}$. This observation is consistent with an increase of turbulence caused by the propagation of the flame in the tube.

A PIV setup is used for the determination of the unburned flow velocity. With this measurement technique, information on the evolution of the turbulence intensity at the top of the prototype over time can also be obtained. This evolution of turbulent intensity is important for modelling validation purpose.

An innovative method for the local measurement of the burning velocity and of the corresponding turbulence level just ahead the flame front has already been proposed Chanut et al. (2020). In this paper, an adaptation of this method is proposed to estimate the global evolution of the burning velocity over time with a global measurement. This global measurement is useful for validation of numerical simulations; while the previous local measurement is useful for estimating the theoretical relation between burning velocity and turbulence intensity. In future tests, this global measurement will be implemented on a same experiment with the local estimation of the burning velocity to compare the results obtained.

Acknowledgments

The authors are grateful to IRSN (Institut de Radioprotection et de Surete Nucléaire) for scientific and financial support to this project.

References

Chanut, C., Heymes, F., Lauret, P., Essaidi, Z., & Slangen, P. (2020a). Visualization of aluminum dust flame propagation in a square-section tube: comparison of schlieren, shadowgraphy and direct visualization techniques. *Journal of Visualization*, *23*(5), 885–894. https://doi.org/10.1007/s12650-020-00676-5

Chanut, C., Heymes, F., Lauret, P., & Lopez, C. (2020b). Experimental determination of aluminum burning velocity during flame propagation in a tube. *Chemical Engineering Transactions*, *82*(December 2019), 205–210. https://doi.org/10.3303/CET2082035

Dahoe, A. E., & de Goey, L. P. H. (2003). On the determination of the laminar burning velocity from closed vessel gas explosions. *Journal of Loss Prevention in the Process Industries*, *16*(6), 457–478. https://doi.org/10.1016/S0950-4230(03)00073-1

Faghih, M., & Chen, Z. (2016). The constant-volume propagating spherical flame method for laminar flame speed measurement. *Science Bulletin*, *61*(16), 1296–1310. https://doi.org/10.1007/s11434-016-1143-6

Goroshin, S., Fomenko, I., & Lee, J. H. S. (1996). Burning velocities in fuel-rich aluminum dust clouds. *Symposium (International) on Combustion*, *26*(2), 1961–1967. https://doi.org/10.1016/S0082-0784(96)80019-1

Julien, P., Whiteley, S., Soo, M., Goroshin, S., Frost, D. L., & Bergthorson, J. M. (2017). Flame speed measurements in aluminum suspensions using a counterflow burner. *Proceedings of the Combustion Institute*, *36*(2), 2291–2298. https://doi.org/10.1016/j.proci.2016.06.150

Kahlili, I. (2012). *Sensibilité, sévérité et spécificités des explosions de mélanges hybrides gaz/vapeurs/poussières*.

Mendez, M. A., Simonini, A., & Spaccapaniccia, C. (2018). *Introduction to Image Velocimetry*. Lecture no. ed. Von Karman Institute.

Proust, C. (2006). Flame propagation and combustion in some dust-air mixtures. *Journal of Loss Prevention in the Process Industries*, *19*, 89–100. https://doi.org/10.1016/j.jlp.2005.06.026